Journal of Power Sources 193 (2009) 885–889

Contents lists available at ScienceDirect

Journal of Power Sources

journal homepage: www.elsevier.com/locate/jpowsour

Short communication

Ag/C nanoparticles as an cathode catalyst for a zinc-air battery with a flowing alkaline electrolyte

Jia-Jun Han, Ning Li*, Tian-Yun Zhang

Department of Applied Chemistry, Harbin Institute of Technology, Harbin 150001, People's Republic of China

ARTICLE INFO

Article history:
Received 15 January 2009
Received in revised form 25 February 2009
Accepted 25 February 2009
Available online 13 March 2009

Keywords:
Ag/C nanoparticle
ORR
Zinc-air battery

ABSTRACT

The cyclic voltammetry indicated that the oxygen reduction reaction (ORR) proceeded by the four-electron pathway mechanism on larger Ag particles (174 nm), and that the ORR proceeded by the four-electron pathway and the two-electron pathway mechanisms on finer Ag particles (4.1 nm), simultaneously. The kinetics towards ORR was measured at a rotating disk electrode (RDE) with Ag/C electrode. The number of exchanged electrons for the ORR was found to be close to four on larger Ag particles (174 nm) and close to three on finer Ag particles (4.1 nm). The zinc-air battery with Ag/C catalysts (25.9 nm) was fabricated and examined.

1. Introduction

The development of fuel cells and metal-air batteries has aroused attention extensively in the world. As the cathode of battery, the oxygen electrode shows poor reversibility and is difficult to reduce, which becomes the major obstacle of battery reaction. How to raise O_2 electrode activity is always one of the focal points in the fuel cell and metal-air battery fields. The overpotential produced by O_2 reduction on the surface of traditional Pt/C catalysts is as high as 300–400 mV, and the performances of the fuel cell and metal-air battery are decreased [1–3]. Besides, Pt electrocatalysts are not only expensive, but also deficient in resource. Less expensive materials of carbon, manganese oxides [4–6] and composite compounds [7–9] are successfully used to replace expensive Pt metal as O_2 electrode catalysts in alkaline medium.

The kinetics and mechanisms of O_2 reduction have been investigated for a wide range of electrode materials and electrolytes. They rely greatly on the choice of active materials [10]. The reduction of O_2 in alkaline electrolytes can be proceeded by two pathways [11], namely:

- Direct O_2 reduction to OH^- ions, what is called four-electron pathway (I):

$$O_2 + 2H_2O + 4e^- \rightarrow 4OH^- \quad \text{(I)}$$

- Or oxygen reduction to HO_2^- ions, what is called two-electron pathway (II):

$$O_2 + H_2O + 2e^- \rightarrow HO_2^- + OH^- \quad \text{(II)}$$

With subsequent reduction of peroxide ion to OH^- ions (III) or the decomposition of peroxide ion (IV):

$$HO_2^- + H_2O + 2e^- \rightarrow 3OH^- \quad \text{(III)}$$

$$2HO_2^- \rightarrow 2OH^- + O_2 + 2e^- \quad \text{(IV)}$$

Ag is one of the typical O_2 reduction catalysts, and has a reasonably high catalytic activity for O_2 reduction in alkaline electrolyte. Furthermore, it is a good catalyst for perhydroxyl ion decomposition [12,13]. Ag was used replacing Pt as O_2 reduction catalysts in fuel cell and metal-air battery in early stage. But Ag particles were easy to accumulate into larger particles in the process of preparation, this would reduce catalytic activity of Ag. Afterwards Ag was adopted rarely. The key to the preparation of Ag catalysts lies in raising the specific surface area of Ag as far as possible [14,15]. Many studies have been reported on the kinetics of O_2 reduction on a bulk Ag electrode, but the ORR seems to vary considerably [14,16–18]. It is reported that the O_2 reduction proceeds by the four-electron pathway mechanism on the surface of the Ag/C electrode [13,14,19]. In the previous work, we synthesized the single crystal of [Ag(L)(bbi)] (L = 2-amino-3,5-dimethylbenzenesulf-onate anion, bbi = 1,1′-(butane-1,4-diyl)diimidazole) [20]. Ag/C catalysts with different contents of Ag were prepared and physically characterized using the [Ag(L)(bbi)] by Ag(I) single crystal reduction method (Ag(I) SCRM). The Ag(I) single crystal reduction is the method of the reduction of Ag(I) ions in single crystals to Ag metal

* Corresponding author. Tel.: +86 631 2679121.
E-mail address: hanjj20032000@yahoo.com.cn (N. Li).

0378-7753/$ – see front matter © 2009 Elsevier B.V. All rights reserved.
doi:10.1016/j.jpowsour.2009.02.082

using $NaBH_4$ as reductant. Their electrochemical performances were investigated by using Ag/C as O_2 reduction electrocatalysts in alkaline electrolyte. The electrocatalytic activity of Ag/C catalysts prepared by Ag(I) SCRM is significantly enhanced compared with that of Ag/C catalysts prepared by Ag_2O reduction method (Ag_2O RM) under the same content of Ag [21]. In this study, the rotating disk electrode (RDE) method and the cyclic voltammetry were used to study the kinetics and mechanism of O_2 electrode reactions, using Ag/C as the catalysts. The performance of the zinc-air battery with Ag/C catalysts prepared by Ag(I) SCRM was examined.

2. Experimental

2.1. Preparation of air electrodes

A rotating disc electrode with a glassy carbon electrode (5 mm diameter) was used. Ag/C catalysts were dispersed in 0.1 wt.% polytetrafluoroethylene (PTFE) solution (Cabot, US) and resultant suspension was agitated in an ultrasonic bath for 30 min. The suspension was coated on the glassy carbon electrode, which was air-dried for 1 h. Ag/C electrodes for a three-electrode cell were prepared. 1.5 g of Ag/C catalysts was weighed and added to 0.5 ml of 50 wt.% PTFE solution, the mixture was mixed fully and pressed into a round sheet of 2.0 cm in diameter. The nickel net was pressed onto one side of the round sheet, and a thin layer of PTFE film was coated evenly on another side. Ag/C electrodes prepared were dried in a vacuum drying oven at 40 °C for 72 h. The cathode of the zinc-air battery was prepared using 10 wt.%Ag/C (25.9 nm) prepared by the Ag(I) SCRM as the catalysts according to the steps detailed in [21]. Ag loading of the cathode was 30 mg cm^{-2}. The carbon support used was VulcanXC-72R carbon (produced by Cabot, US), and its BET area was 254 m^2 g^{-1}.

2.2. Cyclic voltammetry

The reduction of O_2 from air was studied in a three-electrode cell (made of PMMA organic glass) that contained a Pt counter electrode, a Hg/HgO, OH^- reference electrode and a Ag/C electrode as a working electrode. The electrolyte was 5.0 mol L^{-1} KOH aqueous solution. Cyclic voltammograms were conducted with a CHI660A electrochemical workstation system (Shanghai Chenhua Instrument Company). The experiments were performed over the potential range of −0.4 to 1.3 V at a scanning rate of 10 mV s^{-1}.

2.3. Measurement of the kinetics

The kinetics of oxygen reduction was studied in O_2-saturated 1.0 mol L^{-1} KOH solution in a three-electrode cell (made of PMMA organic glass) with the Ag/C glassy carbon electrode as the working electrode, Hg/HgO, OH^- electrode as the reference electrode, and platinum spiral wire as the auxiliary electrode. The electrochemical measurements were performed by the CHI660A electrochemical workstation system (Shanghai Chenhua Instrument Company) and the rotation rates were controlled by the AFMSRXB Model Analytical Rotator (Pine Instrument Company, USA).

2.4. Measurement of the polarization

The anode of the zinc-air battery was an zinc electrode which contained automatic packed cuneiform bed (right inverted trapezoid shaped chamber) made of the nickel mesh. The case of battery was made of PMMA organic glass. The area of the electrode in one side was 5.0 cm × 3.0 cm. The upper slit of the cuneiform trough was 3.0 mm in width and the lower slit was 0.5 mm in width. The zinc grains (1.0 mm diameter) were used as the fuel. Under the action of gravity, the zinc grains automatically entered the cuneiform trough from the upper slit with the flowing electrolyte. The discharge products (ZnO) of zinc were carried by the flowing electrolyte from the lower slit. A schematic diagram of the zinc-air battery is shown in Fig. 1. The polarization data of the battery and electrodes were recorded at a constant current using a LK2000B charge–discharge system (Tianjin LK Company). The flowing alkaline electrolyte was 6.5 mol L^{-1} KOH aqueous solution (2.0 ml min^{-1}) and the reference electrode was a Hg/HgO, OH^- electrode.

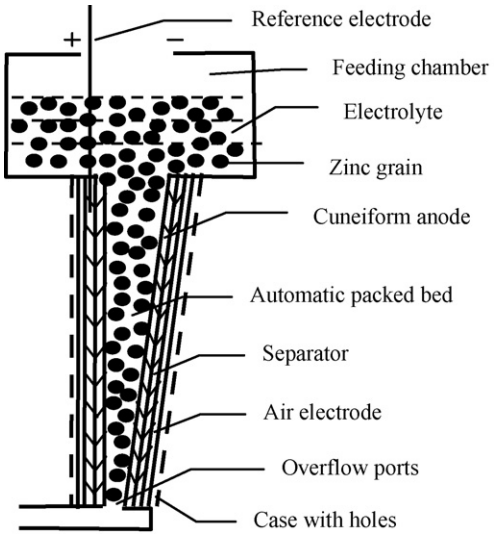

Fig. 1. Schematic diagram of the zinc-air battery.

3. Results and discussions

3.1. Mechanism of the ORR

Cyclic voltammograms were repeated five times for a wide range of potential sweeps for the electrode with 20 wt.%Ag/C catalysts (174 nm) prepared by Ag_2O RM in alkaline electrolyte in Fig. 2. The current peak observed at −0.17 V corresponds to the O_2 reduction reaction. The single reduction potential peak supports the four-electron pathway mechanism.

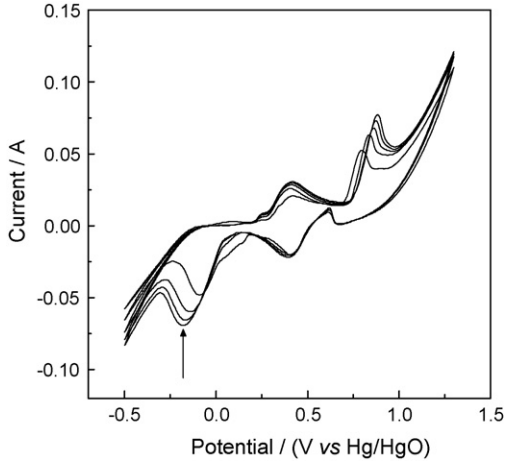

Fig. 2. Cyclic voltammetric curves for O_2 on the electrode with 20 wt.%Ag/C catalysts prepared by Ag_2O RM in 5.0 mol L^{-1} KOH at a scanning rate of 10 mV s^{-1} (the active area of the electrode: 3.0 cm^2; Ag loading: 300 mg).

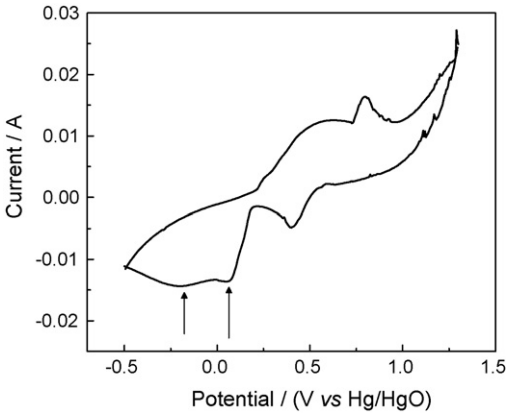

Fig. 3. Cyclic voltammetric curve for O_2 on the electrode with 0.5 wt.%Ag/C catalysts prepared by Ag(I) SCRM in 5.0 mol L^{-1} KOH at a scanning rate of 10 mV s^{-1} (the active area of the electrode: 3.0 cm^2; Ag loading: 7.5 mg).

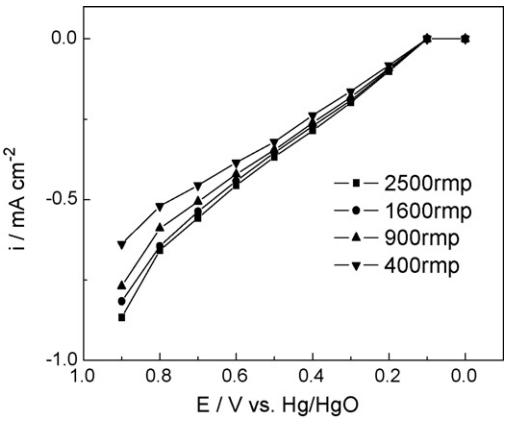

Fig. 4. Curves of the current–potential for O_2 reduction at different rotation rates on a glassy carbon electrode with 20 wt.%Ag/C catalysts prepared by Ag_2O RM in 1.0 mol L^{-1} KOH (the active area of the electrode: 0.2 cm^2; Ag loading: 2 mg).

Fig. 3 shows cyclic voltammogram for the electrode with 0.5 wt.%Ag/C catalysts (4.1 nm) prepared by Ag(I) SCRM in alkaline electrolyte. The current peaks observed at 0.09 and −0.23 V correspond to the O_2 reduction reaction. The two reduction potential peaks support the four-electron pathway and the two-electron pathway mechanisms, simultaneously.

Therefore it can be deduced that the ORR proceeds by the four-electron pathway mechanism on larger Ag particles (174 nm), and that the ORR proceeds by the four-electron pathway and the two-electron pathway mechanisms on finer Ag particles (4.1 nm), simultaneously.

3.2. Kinetic of oxygen reduction

The RDE method was used to study the kinetics of air electrode reaction through a Koutecky–Levich plot. According to the Levich and Koutecky–Levich equations:

$$i_L = 0.620nFAD_0^{2/3}\omega^{1/2}\nu^{-1/6}C_0 \quad (1)$$

$$i_K = nFAK\Gamma_{cat}C_0 \quad (2)$$

$$i^{-1} = i_K^{-1} + i_L^{-1} \quad (3)$$

$$i^{-1} = \frac{1}{(nFAK\Gamma_{cat}C_0)} + \frac{1}{0.620nFAD_0^{2/3}\nu^{-1/6}C_0\omega^{1/2}} \quad (4)$$

where i_L (A) is the limiting current for the electrode reaction of reactive species by the diffusion controlled process, i_K (A) is the kinetic current for the reaction of reactive species at the electrode surface, n (mol^{-1}) is the electron transfer number per mole of reactive species, F (C mol^{-1}) is Faraday constant (=96,500 C mol^{-1}) [22], A (cm^2) is the electrode area, D_0 (cm^2 s^{-1}) is the diffusion coefficient of O_2 in 1 mol L^{-1} KOH solution (=1.76 × 10^{-5} cm^2 s^{-1}) [22], ω (s^{-1}) is the rotation rate, ν (cm^2 s^{-1}) is the kinetic viscosity of water (=0.01 cm^2 s^{-1}) [22], C_0 (mol L^{-1}) is the concentration of O_2 in 1 mol L^{-1} KOH solution at 25 °C (=1.103 × 10^{-3} mol L^{-1}) [22], K (M^{-1} s^{-1}) is the kinetic rate constant for catalytic reaction, and Γ_{cat} (mol cm^{-2}) is the quantity of catalyst on the surface of the electrode (=9.26 × 10^{-5} mol cm^{-2}).

Fig. 4 shows the curves of the current–potential for O_2 reduction at the electrode with 20 wt.%Ag/C catalysts prepared by Ag_2O RM at different rotation rates. The current of O_2 reduction increases with increasing rotation rates. Fig. 5 shows the Koutecky–Levich plots obtained from the data in Fig. 4 .The analysis results of ORR kinetic were summarized in Table 1. The number of exchanged electrons for the ORR was found to be close to four. It is concluded that the ORR is a direct four-electron process. With increasing electrode potential the rate constant increases.

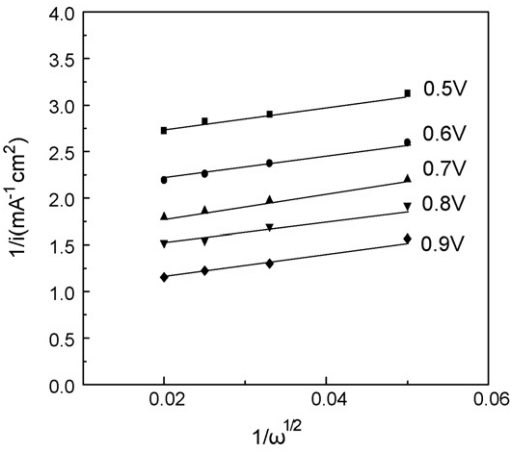

Fig. 5. Koutecky–Levich plots for 20 wt.%Ag/C catalysts prepared by Ag_2O RM at different potentials.

Fig. 6 shows the curves of the current–potential for O_2 reduction at the electrode with 0.5 wt.%Ag/C catalysts prepared by Ag(I) SCRM at different rotation rates. The current of O_2 reduction increases with increasing rotation rates. Fig. 7 shows the Koutecky–Levich plots obtained from the data in Fig. 6. The analysis results of ORR kinetic were summarized in Table 2. The number of exchanged electrons for the ORR was found to be close to three. It is concluded that the ORR proceeds by the four-electron pathway and the two-electron pathway, simultaneously. With increasing electrode potential the rate constant increases.

From Figs. 5 and 7, under the same Ag loadings (2 mg), the current increases with decreasing Ag particle sizes. This indicated that

Table 1
Kinetic parameters for catalytic reduction of oxygen at a glassy carbon electrode with 20 wt.%Ag/C catalysts prepared by Ag_2O RM (Ag loading: 2 mg).

E/V (vs. Hg/HgO, OH^-)	20 wt.%Ag/C catalysts (particle-size of Ag: 174 nm)		
	Slope (×10^3)	n (mol)	K (×10^2 M^{-1} s^{-1})
0.5	5.45	3.80	6.3
0.6	5.57	3.72	7.4
0.7	5.40	3.83	8.6
0.8	5.35	3.87	9.7
0.9	4.97	3.75	10.7

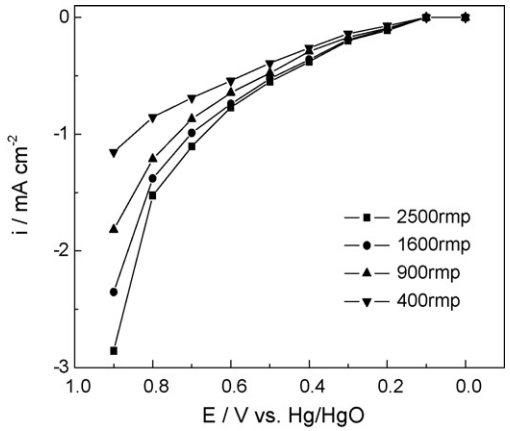

Fig. 6. Curves of the current–potential for O_2 reduction at different rotation rates on a glassy carbon electrode with 0.5 wt.%Ag/C catalysts prepared by Ag(I) SCRM in 1.0 mol L^{-1} KOH (the active area of the electrode: 0.2 cm^2; Ag loading: 2 mg).

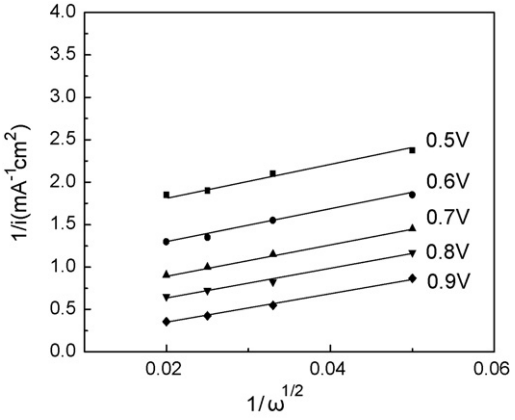

Fig. 7. Koutecky–Levich plots for 0.5 wt.%Ag/C catalysts prepared by Ag(I) SCRM at different potentials.

the electrocatalytic activity was enhanced with increasing specific surface area of Ag.

3.3. Polarization curves of electrodes

Fig. 8 shows the polarization curves of electrodes obtained for the zinc-air battery in the temperature range between 35 °C and 80 °C. The curves indicated that the zinc-air battery is cathode-limited. The polarization of the cathode decreases with increasing temperature. This could be due to the increased reaction kinetics.

3.4. Polarization curves of the battery

Fig. 9 shows the polarization curves of the zinc-air battery obtained at different temperature. With increasing temperature the power density increases. Power densities of 34 mW cm^{-2} at 35 °C and 72 mW cm^{-2} at 80 °C have been obtained.

Table 2
Kinetic parameters for catalytic reduction of oxygen at a glassy carbon electrode with 0.5 wt.%Ag/C catalysts prepared by Ag(I) SCRM (Ag loading: 2 mg).

E/V (vs. Hg/HgO, OH^-)	0.5 wt.%Ag/C catalysts (particle-size of Ag: 4.1 nm)		
	Slope ($\times 10^3$)	n (mol)	K ($\times 10^2$ $M^{-1}s^{-1}$)
0.5	7.03	2.94	18.3
0.6	7.36	2.81	21.4
0.7	7.26	2.85	25.9
0.8	6.90	2.99	38.1
0.9	6.80	2.90	40.9

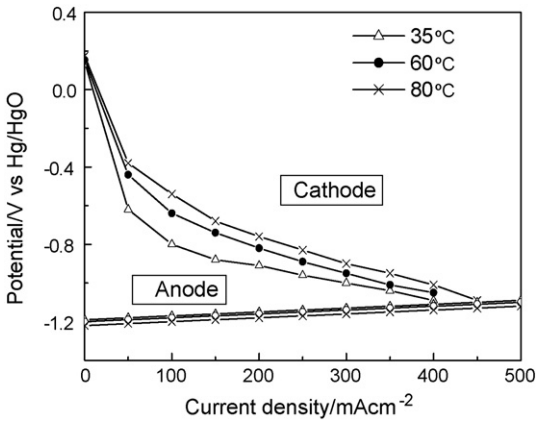

Fig. 8. Polarization curves of the anode and cathode in 6.5 mol L^{-1} KOH (the active area of the electrode: 30 cm^2; Ag loading: 30 mg cm^{-2}; measurement time: 1 min per point).

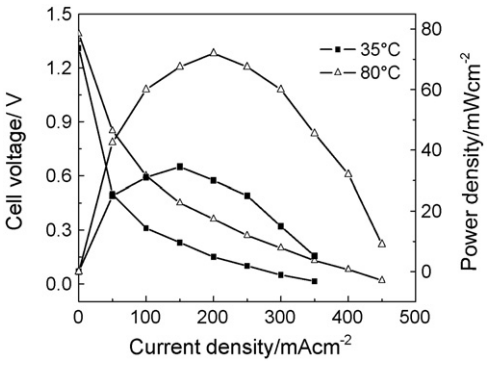

Fig. 9. Polarization curves of the zinc-air battery in 6.5 mol L^{-1} KOH (the active area of the electrode: 30 cm^2; Ag loading: 30 mg cm^{-2}; measurement time: 1 min per point).

4. Conclusions

The ORR proceeds by the four-electron pathway and the two-electron pathway on Ag/C catalysts, simultaneously. The larger Ag particles are favourable to the four-electron reduction of O_2; the finer Ag particles are favourable to the two-electron reduction of O_2. The zinc-air battery has the power densities of 34 mW cm^{-2} at 35 °C and 72 mW cm^{-2} at 80 °C with 10 wt.%Ag/C (25.9 nm) prepared by the Ag(I) SCRM as catalysts.

References

[1] J.-P. Shim, Y.-S. Park, H.-K. Lee, J.-S. Lee, J. Power Sources 74 (1998) 151.
[2] G.J.K. Acres, J. Power Sources 100 (2001) 60.
[3] W.-F. Liu, Q. Tang, B.-L. Yi, H.-M. Zhang, Chin. J. Power Sources 26 (6) (2002) 457.
[4] T.D. Chung, F.C. Anson, J. Electroanal. Chem. 508 (1–2) (2001) 115.
[5] R.P. Kingsborough, T.M. Swager, Chem. Mater. 12 (4) (2000) 872.
[6] J.S. Yang, J.J. Xu, Electrochem. Commun. 5 (4) (2003) 306.
[7] L.M. Ang, T.S.A. Hor, G.Q. Xu, Carbon 38 (3) (2000) 363.
[8] P.C.P. Watts, W.K. Hsu, V. Kotzeva, Chem. Phys. Lett. 366 (1–2) (2002) 42.
[9] X.P. Gao, L. Lan, G.L. Pan, Electrochem. Solid-State Lett. 4 (10) (2001) A173.
[10] V.B. Baez, D. Pletcher, J. Electroanal. Chem. 382 (1–2) (1995) 59.
[11] E. Yeager, J. Mol. Catal. 38 (1986) 5.
[12] E.L. Littauer, K.C. Tsai, J. Electrochem. Soc. 126 (1979) 1924.
[13] G.V. Zhutaeva, N.D. Merkulova, I.N. Landau, Z.G. Garakanidze, V.V. Surikov, J. Appl. Chem. USSR 63 (3) (1990) 522.
[14] S.D. Seliverstov, N.Y. Lyzlov, Z.P. Arkhangelskaya, J. Appl. Chem. USSR 57 (9) (1984) 1824.
[15] P. Fischer, J. Heitbaum, J. Electroanal. Chem. 112 (1980) 231.

[16] D. Sepa, M. Vojnovic, A. Damjanovic, Electrochim. Acta 15 (1970) 1355.
[17] Y.L. Cao, H.X. Yang, X.P. Ai, L.F. Xiao, J. Electroanal. Chem. 557 (2003) 127.
[18] L. Mao, D. Zhang, T. Sotomura, K. Nakatsu, N. Koshiba, T. Ohsaka, Electrochim. Acta 48 (8) (2003) 1015.
[19] B. Miller, J. Electrochem. Soc. 117 (1970) 491.
[20] Jiajun Han, Ning Li, Acta Cryst. E 63 (2007) m1622.
[21] H.A.N. Jia-jun, L.I. Ning, L.I.U. De-li, Chin. J. Power Sources 32 (10) (2008) 673.
[22] R.Z. Jiang, F.C. Anson, J. Electroanal. Chem. 305 (2) (1991) 171.